Rigid Spacecraft Fault-Tolerant Control Using Adaptive Fast Terminal Sliding Mode

Pyare Mohan Tiwari, S. Janardhanan and Mashuq un-Nabi

Abstract In addition to the robustness against inertia uncertainty and external disturbances, the efficient and quick fault-tolerant property is expected by the on-board attitude controller for any spacecraft mission. In comparison to the active fault tolerant control methods, the passive fault-tolerant methods are simpler and require less computation time and power. The finite-time sliding mode using the terminal sliding mode has been proven the efficacy to address the attitude control related issues, but in most of the cases, fault-tolerant issues were not taken into account. The objective of the chapter here is to propose a passive fault-tolerant control by using the finite-time sliding mode control. Firstly, an extensive review has been given to discuss the application of terminal sliding mode and its variants for the attitude control problem. Then, in control design, a non-singular fast terminal sliding mode has been integrated together with the adaptive control, and an adaptive non-singular fast terminal sliding mode control has been designed. In most of the finite time fault-tolerant designed using terminal sliding modes, the controllers gains are remain to constant; which can be cause for chattering. Therefore, to limit the chattering effect, and to avoid the need of upper bounds of uncertainty and external disturbances, adaptive estimate laws have been designed to estimate the controller's gains. Finite time stability has been analyzed by the Lyapunov theorem. Further, to show the fault-tolerance effectiveness of the proposed control law in attitude stabilization and tracking, various simulation results have been presented. The proposed control law is quick, and robust enough to negate the effects of external disturbances, mass inertia uncertainty, and actuator faults.

P.M. Tiwari (✉)
Amity University, Noida, India
e-mail: pmtiwari@amity.edu

S. Janardhanan · Mashuq-un-Nabi
Indian Institute of Technology, New Delhi, India
e-mail: janas@ee.iitd.ac.in

Mashuq-un-Nabi
e-mail: mnabi@ee.iitd.ac.in

A.T. Azar and Q. Zhu (eds.), *Advances and Applications in Sliding Mode Control systems*,
Studies in Computational Intelligence 576, DOI 10.1007/978-3-319-11173-5_14

1 Introduction

Attitude control system (ACS) is an important module in the spacecraft mission design, and in the success of mission, the ACS design plays a vital role. To maintain the efficient performance of ACS, the on-board attitude controller should show the robustness against inertia uncertainty, external disturbances, and actuator fault; and additionally, it is also expected by the attitude controller to ensure the proper attitude stabilization or attitude tracking error reduction, in finite-time.

Sliding mode control (SMC) has considerably used to provide the solution for many non-linear problems (Utkin 1977; John et al. 1993). In this series, in the eighties, SMC application started for the spacecraft attitude control (Vadali 1986). In this continuation , recently, some other works for the rigid spacecraft attitude control have been reported by using the SMC (Yeh 2010; Lu et al. 2013). In these applications of SMC for attitude control design, the sliding surface is of linear structure. The major limitation of SMC is the asymptotic convergence of the system states to equilibrium, and it is due to the linear sliding surface. In conclusion, the SMC attitude control will control the attitude in infinite time.

In the eighties, a new and interesting theory the finite time control (FTC) has been developed (Haimo 1986). In the FTC, it is possible that the system states converge to the respective equilibrium in finite time. Inspired by the FTC theory, researchers have developed the terminal sliding mode (TSM) theory (Venkataraman 1991; Yu and Man 1996; Man and Yu 1997; Tang 1998). In TSM, contrary to the SMC, the sliding surface is the non-linear combination of system states; which ensures the finite time convergence to equilibrium. The application of TSM theory to design the spacecraft attitude control first appeared in Erdong and Zhaowei (2008). The originally proposed TSM suffers with the two drawbacks: one is the singularity in control for some initial condition, and the other is the slower convergence speed when the system states start remotely from the equilibrium. Hence, schemes NTSM (Feng et al. 2002) and FTSM (Yu and Man 2002) have been developed to solve the problem of singularity and convergence speed, respectively. By using the NTSM and FTSM, attitude control laws have been designed in Ding et al. (2009), Li et al. (2011), Lu and Xia (2013) and Tiwari et al. (2010), Zou and Kumar (2011), respectively. To design a control that solves the singularity and the finite time convergence together, non-singular fast terminal sliding mode (NSFTSM) has been developed in Yang et al. (2011). Inspired by NSFTSM Yang et al. (2011), for the attitude stabilization and tracking cases, control laws have been presented in Tiwari et al. (2012) and Tiwari et al. (2014), respectively. In these all the afore-mentioned finite time attitude control references, the actuator fault condition has not been taken into account.

Through the technological advancement, tremendous improvements have been made in the attitude actuators design and their implementation techniques. However, to design a fully autonomous space mission, it is important that the on-board ACS should be able to defeat the actuator fault in finite-time with high speed and efficacy. It is worth mentioning that fault tolerance should be done in finite- time with high speed; otherwise in some specific space missions designed specially for military

applications, the ACS may not be able to maintain the control performance all round. Mainly, the fault tolerant control are categorized in two methods, the active and passive. The active fault tolerant control methods are equipped with fault diagnosis and detection (FDD). The FDD role is to detect and identify the actuator faults; and then to re-configure the controllers to compensate the faults effects. Therefore, obviously that the series of computation and decision steps are required in active fault tolerant method. So, the ACS with active fault tolerant method require more time to complete the online computations; but the long computation time could delay the timely control action, and the control performance may deteriorated to the level that can lead to the catastrophic failures. In contrary to the active methods, the passive fault tolerant control is equipped with the only one controller, and with this controller, both the lumped uncertainty and the actuator faults and saturation are handled. Numerous efforts by taking different control techniques have been reported for the design of passive fault tolerant controllers (Bustan et al. 2013) (and other references mentioned in Bustan et al.).

Inspired by the finite time convergence property of TSM and its variants (NTSM, FTSM, NFTSM), recently, they have been introduced as a qualified passive fault tolerant method for the spacecraft attitude. In Hu et al. (2012), TSM has been applied to compensate the effects of actuator effectiveness loss, inertia uncertainty, and external disturbances. However, the chosen sliding surface suffers with the same limitations as with the originally proposed TSM. The NTSM based fault tolerant control appeared in Hu et al. (2013), Lu et al. (2013). In Hu et al. (2013), finite-time attitude stabilization law under actuator misalignment is addressed. In reference Lu et al. (2013), attitude tracking performance is checked under the actuator fault and effectiveness loss. In these references, the controller gains are remain constant; and gains values are linked with the upper bounds of uncertainty and external disturbance. More than that, to enhance the fault tolerant control quality, recently, the FTSM control and the adaptive control appeared together. In Hu et al. (2012), authors developed the adaptive law updated finite-time controller using FTSM, and applied for the reaction wheel fault tolerance. However, the control law may suffer with limitations of singularity and unbound increment in control gains estimate. In this series, authors of Xiao et al. (2013) have developed the attitude tracking compensation controller, and shown the performance under actuator fault, actuator misalignment, and external disturbances. Though, the recommended controller may cause the singularity problem. In Zhang et al. (2013), by using FTSM, authors have developed the finite-time fault tolerant control; it is shown that together the nominal controller and the adaptive compensation control is successfully accomplished the attitude tracking in the presence of actuator fault and actuator misalignment. In this work also, while discussing the stability proof, the error quaternion vector $e \neq 0$ is considered, but this is not the case always possible. For example, if one of the error quaternion will start or attain value zero, condition $||e^{r-1}|| \leq \ell_3$ will not be fulfilled for $r \in (0, 1)$.

It is noticed that by using TSM and its variants, finite time fault tolerant control is in its early stage; and in the selection of sliding surface, method to decide the controller's gains, and consideration of the different types of faults, are the major areas of improvements in proposing the solution. Our endeavor here is to develop

a control law for the control of rigid spacecraft in the presence of actuator fault, actuator effectiveness loss, external disturbances, uncertain mass inertia parameters. In the control development, the nominal control component is derived by using a non-singular fast terminal sliding mode (NSFTSM) surface. Additionally, to negate the actuator fault and external disturbances as well inertia uncertainty, the nominal controller is supported by the adaptive control component. The closed loop finite time stability has been proved using the Lyapunov stability theory.

The structure of the chapter is as follows: The rigid spacecraft attitude mathematical modeling for stabilization and tracking are discussed in Sect. 2. In Sect. 3 of the chapter discusses the control objective and the proposed fault -tolerant control design with the finite-time stability proof. In Sect. 4, simulation results are illustrated with extensive discussion. Finally, conclusion is given in Sect. 5.

2 System Description

In any space mission, attitude stabilization and tracking are the main aim of ACS. This section discusses the mathematical model for the attitude stabilization as well as for the attitude tracking of a rigid spacecraft. Unit quaternion, due to non-trigonometric expression and non-singularity computation (Wertz 1978), are extensively used parameter to represent the kinematics of a rigid spacecraft; that is why the attitude kinematics is described here by using the unit quaternion.

2.1 Mathematical Model for Attitude Stabilization

Rigid spacecraft attitude control is described by the kinematics and dynamics equations (Wertz 1978). The attitude kinematics representation using the unit quaternion is given as follows.

$$\bar{q} = [q_v^T \quad q_4]^T. \tag{1}$$

where $q_v = [q_1 \quad q_2 \quad q_3]^T = \varepsilon \sin\frac{\theta}{2}$ and $q_4 = \cos\frac{\theta}{2}$ are the vector and the scalar components of the unit quaternion respectively, where $\theta \in \Re$ is the rotation angle about the eigen axis, which is given by the unit vector $\varepsilon = \left[\varepsilon_1 \ \varepsilon_2 \ \varepsilon_3\right]^T$. The scalar and the vector components of unit quaternion satisfies the constraint

$$q_v^T q_v + q_4^2 = 1. \tag{2}$$

The kinematics equations are given as

$$\dot{q_v} = \frac{1}{2}(q_4 I_3 + {q_v}^{\times})\omega$$

$$\dot{q_4} = -\frac{1}{2} q_v^T \omega, \tag{3}$$

where I_3 is the 3×3 identity matrix, $\omega \in \Re^3$ is the the body angular velocity vector measured with respect to the inertial frame expressed in the body frame. The notation $q_v^{\times}$ represents the following skew-symmetric matrix generated by the vector $q_v = [q_1 \quad q_2 \quad q_3]^T$

$$q_v{}^{\times} = \begin{bmatrix} 0 & -q_3 & q_2 \\ q_3 & 0 & -q_1 \\ -q_2 & q_1 & 0 \end{bmatrix}$$

The dynamics equation for a rigid body spacecraft is given by

$$\dot{\omega} = J^{-1}(-\omega^{\times} J\omega + D\, \Delta(t)\, u(t) + d(t)) \tag{4}$$

where $J = J_0 + \delta J$ is the inertia matrix of spacecraft, where $J_0 \in \Re^{3\times 3}$ and $\delta J \in \Re^{3\times 3}$ are the nominal component and the uncertain components respectively, $u(t) \in \Re^n$ is the control input generated by n actuators, $D \in R^{3\times n}$ is the actuator distribution matrix, and $d(t) \in \Re^3$ is the bounded external disturbance torque acting on the body, $\Delta(t) = diag(\Delta_1,\ \Delta_2,\ \Delta_3, ...,\ \Delta_n) \in \Re^{n\times n}$ is the actuator effectiveness matrix with $0 \leq \Delta_i \leq 1$. Important to note that $\Delta_i = 1$ means that particular actuator is fully healthy, and $\Delta_i = 0$ means particular actuator is lost its strength completely, and if $\Delta_i < 1$, then particular actuator is partially functioning. The notation $\omega^{\times}$ is a skew-symmetric matrix generated by ω.

2.2 Mathematical Model for Attitude Tracking

To define the attitude kinematics and dynamics equation for tracking control problem, the relative attitude error between reference frame and a desired reference frame is required to be established. The error quaternion $q_e = [q_{ev}^T,\ q_{e4}]^T \in \Re \times \Re^3$ and the angular velocity error $\omega_e \in \Re^3$ are measured from body fixed reference frame to the desired reference frame, and the defining equations are as follows

$$\begin{aligned} q_{ev} &= q_{d4} q_v - q_{dv}^{\times} q_v - q_4 q_{dv} \\ q_{e4} &= q_{dv}^T q_v + q_4 q_{dv} \\ \omega_e &= \omega - C\omega_d, \end{aligned} \tag{5}$$

where $q_{ev} = [q_{e1} \quad q_{e2} \quad q_{e3}]^T$ and q_{e4} are the vector and scalar components of the error quaternion, respectively, $q_{dv} = [q_{d1} \quad q_{d2} \quad q_{d3}]^T \in \Re^3$, $q_{d4} \in \Re$, and $\omega_d = [\omega_{d1} \quad \omega_{d2} \quad \omega_{d3}]^T \in \Re^3$ are the desired attitude frame vector quaternion, scalar quaternion, and angular velocity, respectively. Both q_e and $q_d =$

$[q_{d1} \quad q_{d2} \quad q_{d3} \quad q_{d4}]^T$ satisfy the constraint $q_{ev}^T q_{ev} + q_{e4}^2 = 1$ and $q_{dv}^T q_{dv} + q_{d4}^2 = 1$; respectively. $C = (q_{e4}^2 - 2q_{ev}^T)I + 2q_{ev}q_{ev}^T - 2q_{e4}q_{ev}^\times \in \Re^{3\times 3}$ with $||C|| = 1$ and $\dot{C} = -\omega^\times C$ represents the rotation matrix between body fixed reference frame and desired reference frame.

Then, using (5), the attitude kinematics and the dynamics equation for the tracking problem could be written as

$$\begin{aligned} \dot{q}_{ev} &= \frac{1}{2}(q_{e4}I + q_{ev}^\times)\omega_e \\ \dot{q}_{e4} &= -\frac{1}{2}q_{ev}^T\omega_e \end{aligned} \tag{6}$$

$$\dot{\omega}_e = J^{-1}\left((-\omega_e + C\omega_d)^\times J(\omega_e + C\omega_d) + J(\omega_e^\times C\omega_d - C\dot{\omega_d}) + D\,\Delta(t)\,u(t) + d(t)\right). \tag{7}$$

3 Fault Tolerant Control Design

In this section, first the control objective is defined, and then the control design method is developed by using a non-singular fast terminal sliding mode. To compensate the effects of actuator fault, external disturbances, and inertia matrix uncertainty, an adaptive control component is applied with nominal control. The proposed fault-tolerant control design will be completed in following three steps

1. Selection of sliding surface
2. Control structure
3. Stability proof both in reaching phase and in sliding phase.

3.1 Control Objective

The control objective is to design a robust fault tolerant controller that to ensure the finite time attitude control in presence of external disturbance, inertia uncertainty, loss of actuator effectiveness, and any fault. Mathematical representation for the control objective is

$$\begin{cases} \lim\limits_{t\to t_f}(q_v - q_d) = 0 \\ \lim\limits_{t\to t_f}\Omega = 0, \end{cases} \tag{8}$$

where $\Omega = (\omega - \omega_d) \in \Re^3$.

In the fore coming control design to achieve the afore-mentioned control objective, the following assumptions are made.

Assumption 1 The body frame quaternion q and angular velocity ω are measurable, and available for feedback.

Assumption 2 The desired reference attitude frame angular velocity ω_d and its first time derivative $\dot{\omega_d}$ are bounded.

Assumption 3 Spacecraft mass inertia matrix nominal component J_0 and the uncertain component δJ are bounded; though the bound limits are not known in advance.

Assumption 4 The control input is not unlimited, and constrained by the limit $u(t) \leq u_{max}$.

Assumption 5 External disturbance $d(t)$ is bounded, and the bound limit is not known in advance.

3.2 Control Design

The detailed design steps are as under

Step 1: Sliding surface design

In contrary to the published finite-time fault tolerant control, here the sliding surface is chosen that to avoid the singularity and to get quick convergence speed. Therefore, using the angular velocity error and the quaternion error information the sliding surface selected is

$$\sigma_e = sig^{\alpha}(\omega_e) + M_1 sig^{\alpha}(q_{ev}) + M_2(q_{ev}) \tag{9}$$

here, $\sigma_e \in \Re^3$ is the sliding surface chosen, $\alpha \in (1, 2)$, $M_1 = diag(m_{11}, m_{12}, m_{13})$, $M_2 = diag(m_{21}, m_{22}, m_{23})$ with $m_{ij} \in \Re$ for $i = 1, 2$ and $j = 1, 2, 3$, and for any vector $y \in \Re^3$, the notation $sig^{\alpha}(y) = [|y_1|^{\alpha} sign(y_1) \quad |y_2|^{\alpha} sign(y_2) \quad |y_3|^{\alpha} sign(y_3)]$.

Now, evaluating

$$\begin{aligned} J\dot{\sigma_e} = {} & \alpha diag(|\omega_e|^{\alpha-1}) J\dot{\omega_e} \\ & + \frac{J}{2}(M_1 \alpha diag(|q_{ev}|)^{\alpha-1} + M_2)(q_{e4} I_3 + q_{ev}^{\times})\omega_e \end{aligned} \tag{10}$$

Applying (7) in (10), we have

$$\begin{aligned} J\dot{\sigma_e} = {} & \alpha diag(|\omega_e|^{\alpha-1}) \Big((-\omega_e + C\omega_d)^{\times} J_o(\omega_e + C\omega_d) + J_o(\omega_e^{\times} C\omega_d - C\dot{\omega_d}) \\ & + D\,\Delta(t)\,u(t) + d(t) + L(q_e, \omega_e, \omega_d, \dot{\omega}_d, \delta J) \Big) + \frac{J_o}{2}(M_1 \alpha diag(|q_{ev}|)^{\alpha-1} \\ & + M_2)(q_{e4} I_3 + q_{ev}^{\times})\omega_e \end{aligned} \tag{11}$$

where $L(q_e, \omega_e, \omega_d, \dot{\omega}_d, \delta J) = (-\omega_e + C\omega_d)^{\times}\delta J(\omega_e + C\omega_d) + \delta J(\omega_e^{\times} C\omega_d - C\dot{\omega}_d) + \frac{\delta J}{2\alpha}(M_1 \alpha diag(|q_{ev}|)^{\alpha-1} + M_2)(q_{e4} I_3 + q_{ev}^{\times}) sig^{2-\alpha}(\omega_e)$ represents the uncertain terms due to inertia matrix uncertainty.

Step 2: Control structure

To achieve the desired control objective (8), the proposed control structure is given as follows

$$u(t) = u_{nom}(t) + u_{ada}(t) \tag{12}$$

where

$$u_{nom}(t) = D^{\dagger}\Big((\omega_e + C\omega_d)^{\times} J_o(\omega_e + C\omega_d) - J_o(\omega_e^{\times} C\omega_d - C\dot{\omega}_d) - \frac{J_o}{2\alpha}(M_1 \alpha diag(|q_{ev}|^{\alpha-1}) + M_2)(q_{e4} I_3 + q_{ev}^{\times}) sig^{2-\alpha}\omega_e\Big) \tag{13}$$

and

$$u_{ada}(t) = \begin{cases} D^{\dagger}(-\hat{k}_1 \sigma_e - \hat{k}_2 sig^{\gamma}(\sigma_e)), & \text{if } ||\sigma_e|| \geq \varepsilon \\ 0, & \text{if } ||\sigma_e|| < \varepsilon, \end{cases} \tag{14}$$

where $D^{\dagger} = D^T(D\,D^T)^{-1}$ is a right-pseudo inverse of actuator distribution matrix D, $\hat{k}_1$ and $\hat{k}_2$ are the estimates of controller gains k_1 and k_2, respectively.

The adaptive estimate laws proposed here are as follows

$$\dot{\hat{k}}_1 = \begin{cases} \alpha\ \eta ||\omega_e^{\alpha-1}||_{\infty}\ ||\sigma_e||^2, & \text{if } ||\sigma_e|| \geq \varepsilon \\ 0, & \text{if } ||\sigma_e|| < \varepsilon, \end{cases} \tag{15}$$

$$\dot{\hat{k}}_2 = \begin{cases} \alpha\ \theta ||\omega_e^{\alpha-1}||_{\infty}\ ||\sigma_e||_{\gamma+1}^{\gamma+1}, & \text{if } ||\sigma_e|| \geq \varepsilon \\ 0, & \text{if } ||\sigma_e|| < \varepsilon, \end{cases} \tag{16}$$

where, $\eta \in \Re, \theta \in \Re, \varepsilon \in \Re$ are the design parameters, and $||\sigma_e||_{\gamma+1}^{\gamma+1} = [|\sigma_{e1}|^{\gamma+1} + |\sigma_{e2}|^{\gamma+1} + |\sigma_{e3}|^{\gamma+1}]^{\gamma+1}$.

Remark 1 The nominal component of the proposed controller is evaluated by applying the invariance principle. Obviously, the nominal control expression, (13) have two terms with the fractional power, but both powers are nonnegative and hence there is no point of singularity.

Remark 2 To negate the effects of inertia uncertainty and external disturbance, and to accelerate the convergence speed in reaching phase, an adaptive control component is added with the nominal control. In most of the published fault tolerant control, the controller's gains are static, and are decided on the basis of uncertainty and disturbance upper bounds, but practically it is difficult to know the bounds in advance.

Therefore, here to estimate the gains values, adaptive estimate laws are proposed. From (15) and (16), it is notable that the adaptive estimate laws depend on only the system states, and not to the uncertainty, disturbance, and actuator faults. Further, to reject the possibility of unbound growth in the controller's gains, dead zone technique has been applied. It is evident from (14), (15), and (16), that both the adaptive control and the adaptive gains will not be updated once the attitude states reach into the desired boundary.

Remark 3 In the proposed adaptive laws, parameters η and θ are working to regulate the estimate speed. Higher the values of η and θ, higher the convergence speed for $\sigma_e = 0$ is obtained.

Step 3: Stability Analysis

The finite time stability check of closed loop system (6)–(7) is completed in two steps. In first step, the reaching phase stability is proved, and in second step the sliding phase stability is proved. Before the stability discussion, the following lemma, discussing the finite-time stability is useful.

Lemma 1 (Yu et al. 2005) *An extended Lyapunov description of finite-time stability with faster finite time convergence can be given as*

$$\dot{V}(x) + \lambda_1 V(x) + \lambda_2 V^m(x) \leq 0 \tag{17}$$

and the convergence time can be given as

$$t \leq \frac{1}{\lambda_1(1-m)} ln \frac{\lambda_1 V^{1-m}(x_0) + \lambda_2}{\lambda_2} \tag{18}$$

where $\lambda_1 > 0$, $\lambda_2 > 0$, *and* $m \in (0, 1)$.

Reaching phase stability

Theorem 1 *With the controller* (12)*, the attitude states of* (6)–(7) *will be able to reach the neighborhood of* $\sigma_e = 0$ *in finite time.*

Proof Select the Lyapunov function

$$V_1 = \frac{1}{2}\sigma_e^T J \sigma_e + \frac{1}{2\eta}\bar{k}_1^2 + \frac{1}{2\theta}\bar{k}_2^2 \tag{19}$$

where, $\bar{k}_1 = \hat{k}_1 - k_1$ and $\bar{k}_2 = \hat{k}_2 - k_2$, and V_1 satisfies

$$\frac{1}{2}\lambda_{min}(J)||\sigma_e||^2 \leq \frac{1}{2}\lambda_{max}(J)||\sigma_e||^2 \tag{20}$$

Taking the first time derivative V_1, and applying (11) leads to

$$\dot{V}_1 = \sigma_e^T \Big(\alpha \, diag(|\omega_e|^{\alpha-1}) \Big((-\omega_e + C\omega_d)^{\times} J_o(\omega_e + C\omega_d) + J_o(\omega_e^{\times} C\omega_d - C\dot{\omega_d}) + D\,u(t) + D\,(\Delta - I_4)u(t) + d(t) + L(q_e, \omega_e, \omega_d, \dot{\omega}_d, \delta J) \Big) \Big) + \frac{1}{\eta}(\hat{k}_1 - k_1)\dot{\hat{k}}_1 + \frac{1}{\theta}(\hat{k}_2 - k_2)\dot{\hat{k}}_2 \tag{21}$$

Further, defining $\bar{L} = D\,(\Delta - I_4)u(t) + d(t) + L(q_e, \omega_e, \omega_d, \dot{\omega}_d, \delta J)$, and then it could be written that

$$||\bar{L}|| \leq ||\bar{L}||_1 \leq ||D\,(\Delta - I_4)u(t)||_1 + ||d(t)||_1 + ||L||_1 \tag{22}$$

and then substituting (12)–(16), (22); and (21) yields

$$\begin{aligned}
\dot{V}_1 &= \sigma_e^T \alpha diag(|\omega_e|^{\alpha-1}) \Big(-\hat{k}_1\sigma_e - \hat{k}_2 sig^{\gamma}(\sigma_e) + \bar{L} \Big) \\
&\quad + \alpha(\hat{k}_1 - k_1)||\,|\omega_e^{\alpha-1}|\,||_\infty\,||\sigma_e||^2 + \alpha(\hat{k}_2 - k_2)||\omega_e^{\alpha-1}||_\infty||||\sigma_e||_{\gamma+1}^{\gamma+1} \\
&\leq -\alpha\hat{k}_1|||\omega_e|^{\alpha-1}||_\infty\,||\sigma_e||^2 - \alpha\hat{k}_2|||\omega_e|^{\alpha-1}||_\infty\,||\sigma_e||_{\gamma+1}^{\gamma+1} + \alpha||\bar{L}||\,|||\omega_e|^{\alpha-1}||_\infty||\sigma_e^T|| \\
&\quad + \alpha(\hat{k}_1 - k_1)||\omega_e^{\alpha-1}||_\infty||\sigma_e||^2 + \alpha(\hat{k}_2 - k_2)||\omega_e^{\alpha-1}||_\infty||\,||\sigma_e||_{\gamma+1}^{\gamma+1} \\
&\leq -\alpha k_1|||\omega_e|^{\alpha-1}||_\infty||||\sigma_e||^2 - \alpha k_2|||\omega_e|^{\alpha-1}||_\infty\,||\,||\sigma_e||_{\gamma+1}^{\gamma+1} \\
&\quad + \alpha||\bar{L}||\,|||\omega_e|^{\alpha-1}||_\infty\,||\sigma_e^T||
\end{aligned} \tag{23}$$

In reaching phase ($\sigma_e \neq 0$), it is easy to show that $\omega_e = 0$ is not an attractor (Appendix). Therefore, (23) can be rewritten in the following two forms:

$$\dot{V}_1 \leq -\frac{2\alpha|||\omega_e|^{\alpha-1}||_\infty}{\lambda_{max}(J)}\left(k_1 - \frac{||\bar{L}||}{||\sigma_e||}\right)V_1 - \left(\frac{2}{\lambda_{max}(J)}\right)^{\frac{\gamma+1}{2}} \alpha k_2|||\omega_e|^{\alpha-1}||_\infty V_1^{\frac{\gamma+1}{2}} \tag{24}$$

$$\dot{V}_1 \leq -\frac{2\alpha k_1|||\omega_e|^{\alpha-1}||_\infty}{\lambda_{max}(J)}V_1 - \left(\frac{2}{\lambda_{max}(J)}\right)^{\frac{\gamma+1}{2}} \alpha|||\omega_e|^{\alpha-1}||_\infty\left(k_2 - \frac{||\bar{L}||\,||\sigma_e||}{||\sigma_e||_{\gamma+1}^{\gamma+1}}\right)V_1^{\frac{\gamma+1}{2}} \tag{25}$$

The stability analysis of (24) and (25) are completed in two scenario.

1. **Scenario1** ($d(t) = 0$), $\delta J = 0$, $\Delta = I_4$)

   In this scenario, both (24) and (25) are simplified to $\dot{V}_1 + \Gamma_1 V_1 + \Gamma_2 V_1^{\frac{\gamma+1}{2}}$, where $\Gamma_1 = \frac{2\alpha k_1|||\omega_e|^{\alpha-1}||_\infty}{\lambda_{max}(J)}$, $\Gamma_2 = \left(\frac{2}{\lambda_{max}(J)}\right)^{\frac{\gamma+1}{2}} \alpha k_2|||\omega_e|^{\alpha-1}||_\infty$, and therefore,

convergence to $\sigma_e = 0$ is ensured in finite time

$$t_1 \leq \frac{1}{\Gamma_1(1-\gamma)/2} \ln \frac{\Gamma_1 V_2^{(1-\gamma)/2}(\sigma_e(0)) + \Gamma_2}{\Gamma_2}. \tag{26}$$

2. **Scenario2** ($d(t) \neq 0$), $\delta J \neq 0$, $\Delta \neq I_4$)
Following the analysis given in Yu et al. (2005), from (24) and (25) it is obvious that, if $k_1 - \frac{||\bar{L}||}{||\sigma_e||} > 0$ and $k_2 - \frac{||\bar{L}||\,||\sigma_e||}{||\sigma_e||_{\gamma+1}^{\gamma+1}} > 0$ is ensured, then (24) and (25) structure will take the faster finite time stability condition (17) of Lemma 1, and the region $||\sigma_e|| < \frac{||\bar{L}||}{k_1}$ and $||\sigma_e|| < \left(\frac{||\bar{L}||}{k_2}\right)^{1/\gamma}$ will be achieved in finite time, respectively. This completes the proof.

Sliding phase stability

Theorem 2 *After the attitude trajectory of system (6)–(7) reach to the neighborhood of $\sigma_e = 0$, the tracking error in attitude states will converge to zero in finite time.*

Proof Once the attitude states of (6)–(7) reach to $\sigma_e = 0$, we have

$$\begin{aligned} sig^{\alpha}(\omega_e) + M_1\, sig^{\alpha}(q_{ev}) + M_2\, q_{ev} &= 0 \\ \omega_e \leq -M_1^{\frac{1}{\alpha}} q_{ev} - M_1^{\frac{1}{\alpha}} sig^{\frac{1}{\alpha}} q_{ev} \end{aligned} \tag{27}$$

Define another Lyapunov function

$$V_2 = q_{ev}^T q_{ev}. \tag{28}$$

Evaluating the first time derivative of (28), give

$$\begin{aligned} \dot{V}_2 &= 2q_{ev}^T \dot{q}_{ev} \\ &= q_{ev}^T (q_{e4} I + q_{ev}^{\times}) \omega_e. \end{aligned} \tag{29}$$

Applying the inequality (27), and using the fact $||(q_{e4} I + q_{ev}^{\times})|| \leq 1$, the above expression results

$$\begin{aligned} \dot{V}_2 &\leq q_{ev}^T (-M_1^{1/\alpha}(q_{ev}) - M_2^{1/\alpha} sig^{1/\alpha}(q_{ev})) \\ &\leq -M_1^{1/\alpha} V_2 - M_2^{1/\alpha} V_2^{(\alpha+1)/2\alpha} \\ &\leq -\lambda_1 V_2 - \lambda_2 V_2^{(\alpha+1)/2\alpha} \end{aligned} \tag{30}$$

where λ_1 and λ_2 are the minimum eigen values of $M_1^{1/\alpha}$ and $M_2^{1/\alpha}$, respectively. Therefore,

$$\dot{V}_2 + \lambda_1 V_2 + \lambda_2 V_2^{(\alpha+1)/2\alpha} \leq 0 \tag{31}$$

The above Eq. (31) satisfies the finite time stability criteria (17), and hence, once the attitude trajectory falls on to the sliding surface, then the quaternion error will converge to zero in finite time

$$t_2 \leq \frac{1}{\lambda_1(\alpha-1)/2\alpha} \ln \frac{\lambda_1 V_2^{(\alpha-1)/2\alpha}(\sigma_e(t_1)) + \lambda_2}{\lambda_2}, \tag{32}$$

where t_1 is the time to cross the reaching phase and to enter into the neighborhood region of $\sigma_e = 0$. Subsequently, by (6), it is proved that $\omega_e = 0$. This completes the proof.

Remark 4 From (32), it is obvious that M_1 and M_2 both have significant effect on the convergence speed. However, the nominal control component (13) is also linked with M_1 and M_2. Therefore, it is desired that while deciding M_1 and M_2, both the convergence speed and the control input level should be monitored.

4 Simulation and Result Discussion

In this section, to verify the effectiveness of the proposed control method, simulations are conducted and the outcomes are presented with extensive discussion. The proposed controller effectiveness demonstration completes in two steps. In the first step, a small spacecraft attitude stabilization performance for the pure condition ($d(t) = 0$, $\delta J = 0, \Delta = 0$), and the practical condition ($d(t) \neq 0, \delta J \neq 0, \Delta \neq 0$) is checked. In the second step, a practical spacecraft is taken, and its attitude tracking performance is demonstrated for practical conditions. Other than the structural difference and type of control, the both simulation steps differs on certain other grounds. In stabilization example, number of actuators are four, and in tracking example three actuators are applied. Additionally, in the tracking example, both the additive fault and actuator effectiveness loss are applied.

4.1 Step 1: Spacecraft Attitude Stabilization

The considered spacecraft parameters are referred from Hu et al. (2012). The nominal component and the uncertain component of spacecraft inertia matrix are $J_o = [20\,0\,0.9;\ 0\,17\,0;\ 0.9\,0\,15]$ and $\delta J = diag[3,\ 2,\ 1][1 + e^{-0.1t} + 2\Upsilon(t-10) - 4\Upsilon(t-20)]$, respectively, where $\Upsilon(x) = 1$ for $x \geq 0$, else $\Upsilon(x) = 0$. The spacecraft attitude is controlled with four reaction wheels with torque constraint limit $|u(t)| \leq 0.2$ N-m; the distribution matrix for reaction wheels is

$$D = \begin{bmatrix} -1 & 0 & 0 & 1/\sqrt{3} \\ 0 & -1 & 0 & 1/\sqrt{3} \\ 0 & 0 & -1 & 1/\sqrt{3} \end{bmatrix}.$$

For the simulations, rigid spacecraft mathematical model discussed in (6)–(7) is used. The initial conditions of the body frame quaternion and the body frame angular velocity are taken as $q_v(0) = [0.3 \ -0.2 \ -0.3 \ 0.8832]^T$ and $\omega(0) = [0 \ 0 \ 0]^T$, respectively. The desired frame is characterized with $q_d(0) = [0 \, 0 \, 0 \, 1]^T$ and $\omega_d(0) = [0 \ 0 \ 0]^T$.

Further, to check the robustness against external disturbances, and to investigate the proposed controller effectiveness against actuator faults, the following mathematical model for the external disturbance and the actuator fault, respectively, are taken (Hu et al. 2012).

External disturbance:

$$d(t) = (||\omega||^2 + 0.005)[sin\ 0.8t\ cos\ 0.5t\ cos\ 0.3t]^T N - m \tag{33}$$

Actuator effectiveness:

$$\Delta_1 = \begin{cases} 1, & \text{if } t \leq 2.4\,\text{s}. \\ 0.45 + 0.15\ rand(t_i) + 0.1sin(0.5t + \pi/3), & \text{if } t > 2.4\,\text{s}. \end{cases}$$

$$\Delta_2 = \begin{cases} 1, & \text{if } t \leq 5.0\,\text{s}. \\ 0.50 + 0.15\ rand(t_i) + 0.1sin(0.5t + 2\pi/3), & \text{if } t > 5.0\,\text{s}. \end{cases}$$

$$\Delta_3 = \begin{cases} 1, & \text{if } t \leq 10.0\,\text{s}. \\ 0.40 + 0.15\ rand(t_i) + 0.1sin(0.5t + \pi), & \text{if } t > 10.0\,\text{s}. \end{cases}$$

$$\Delta_4 = \begin{cases} 1, & \text{if } t \leq 15.0\,\text{s}. \\ 0, & \text{if } t > 15.0\,\text{s}. \end{cases} \tag{34}$$

The controller settings used for the stabilization are mentioned in Table 1.

4.1.1 Interpretation and Discussion with Comparative Comments on Stabilization Performance

Case 1: Stabilization performance for pure condition

For the pure condition, simulation results are shown in Figs. 1, 2 and 3. The top and bottom frames of Fig. 1a illustrate that the error quaternion and the angular velocity error vectors, respectively, reduces to zero in finite time. Figure 1b illustrates the steady precision of the error quaternion and angular velocity error vectors. Figure 2 depicts the time evolution of the NSFTSM vector and the control input; in which the bottom frame of Fig. 2a illustrates that the control input is continuous. The steady

Table 1 Controller parameters

Step 1	Attitude stabilization	$M_1 = diag(0.080,\ 0.080,\ 0.080)$ $\alpha = 1.1$ $k_1(0) = 1.5$ $\eta = 30$	$M_2 = diag(0.152,\ 0.152,\ 0.152)$ $\gamma = 0.47$ $k_2(0) = 0.20$ $\phi = 25$
Step 2	Attitude tracking	$M_1 = diag(0.07,\ 0.07,\ 0.07)$ $\alpha = 1.1$ $k_1(0) = 0.80$ $\eta = 60$	$M_2 = diag(2.90,\ 2.90,\ 2.90)$ $\gamma = 0.49$ $k_2(0) = 0.02$ $\phi = 56$

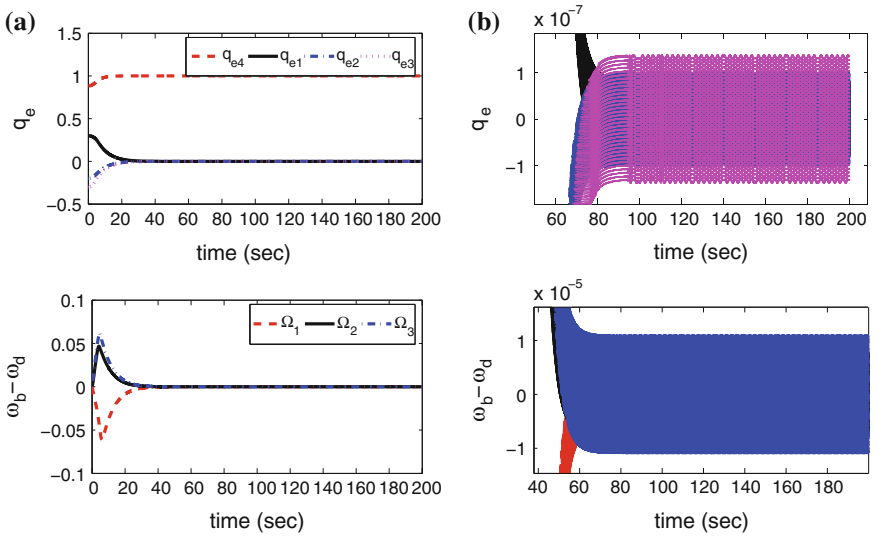

Fig. 1 Stabilization performance Case 1: quaternion and angular velocity pattern under pure condition. **a** Quaternion and angular velocity. **b** Steady precision

precision of NSFTSM vector and control input are illustrated in Fig. 2b. Figure 3 illustrates the estimates of control gains.

As illustrated in Figs. 1 and 2 and mentioned in Table 2, the proposed controller needs time 5.8 s to guarantee that the NSFTSM vector entered into the band $|\sigma_e| \leq 5e-3$; and further, total time 18.15 s is required to satisfy the condition $(|q_{ev}|, |\Omega|) \leq 2e-2$. Additionally, it is revealed that the steady precision for the error quaternion vector, the angular velocity error vector, and the NSFTSM vector are ensured in the range $|q_{ev}| \leq 1.35e-7$, $|\Omega| \leq 1.07e-5$, $|\sigma_e| < 3.41e-6$, respectively.

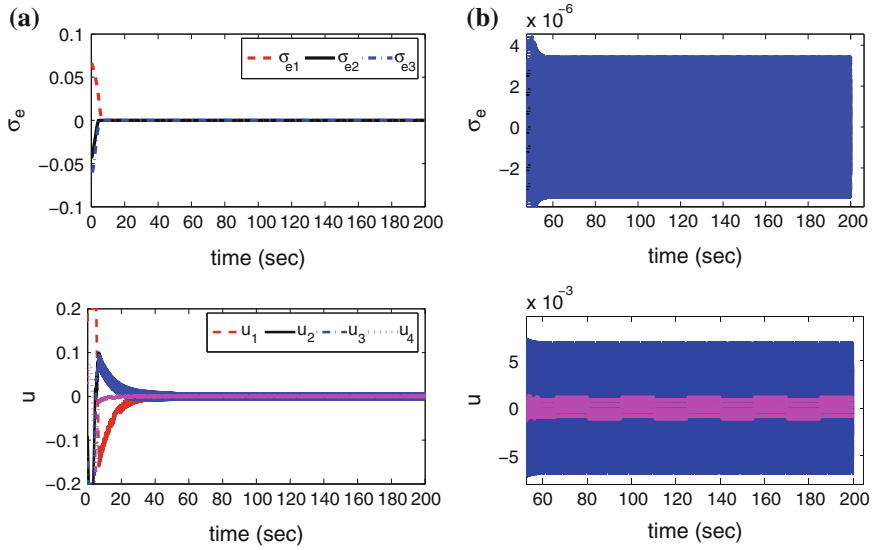

Fig. 2 Stabilization performance Case 1: sliding vectors and control input pattern under pure condition. **a** Sliding vectors and control input. **b** Steady precision

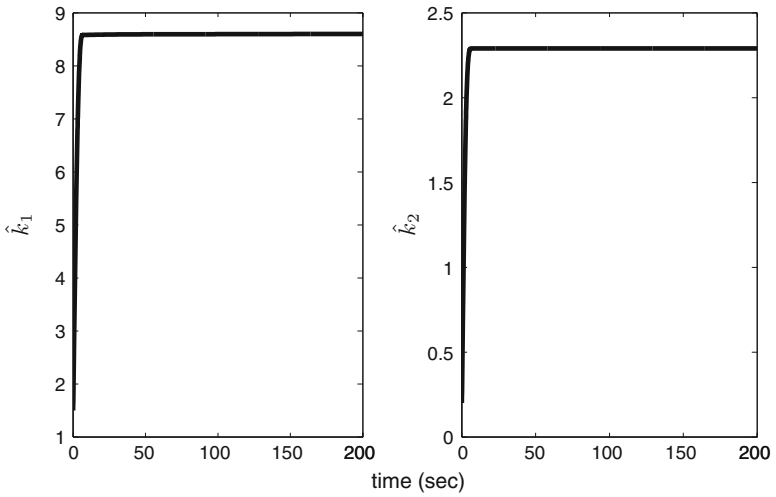

Fig. 3 Stabilization performance Case 1: estimate of control gains

Case 2: Stabilization performance for practical condition

Further, the spacecraft stabilization performance is verified with inertia uncertainty, external disturbance (33), and loss of actuator effectiveness (34). The simulation results are illustrated in Figs. 4 and 6. In Fig. 4a, the finite time convergence of the quaternion and the angular velocity to the desired level, respectively, are portrayed.

Table 2 Controller performance summary

Controller	Control type	Steady precision			Convergence time (in s) for	
		σ_e	q_{ev}	Ω	$\lvert\sigma_e\rvert <$ 5e-3	$(\lvert q_{ei}\rvert, \lvert\Omega_i\rvert) <$ (2e-2,2e-2)
(12): Case 1	Stabilization	$\pm 3.41e$-6	$\pm 1.35e$-7	$\pm 1.07e$-5	5.8	18.15
(12): Case 2	Stabilization	$\pm 2.62e$-5	$\pm 6.26e$-5	$\pm 5.26e$-5	8.05	20.9
(22)(Hu et al. 2012): Case 2	Stabilization	$\pm 9.83e$-4	$\pm 3.11e$-5	$\pm 9.51e$-4	36.81	35.42
(12)	Tracking	$\pm 6.62e$-4	$\pm 8.80e$-4	3.66e-5	14.81	13.15
(13)(Lu et al. 2013)	Tracking	$\pm 2.74e$-5	$\pm 6.25e$-4	$\pm 3.35e$-5	30.34	29.06

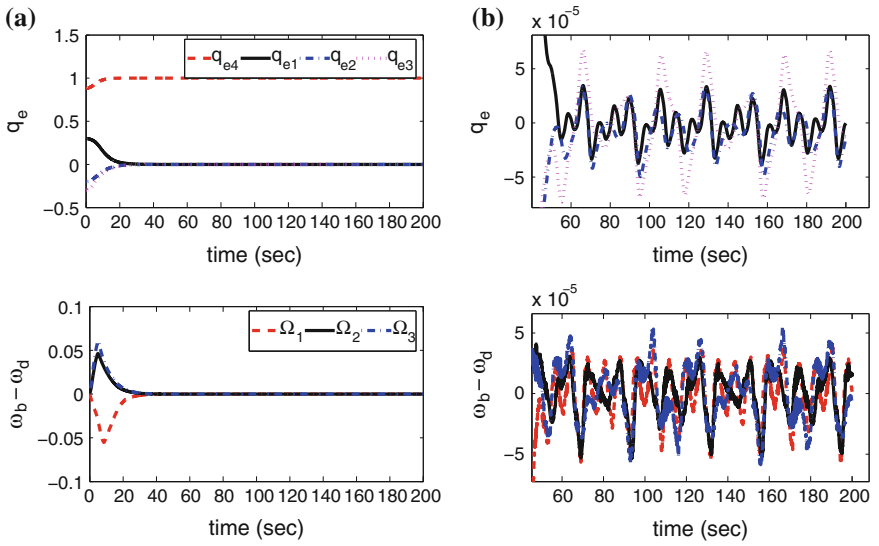

Fig. 4 Stabilization performance Case 2: quaternion and angular velocity pattern under uncertainty, disturbance, actuator fault. **a** Quaternion and angular velocity. **b** Steady precision

It is verified that even with the presence of uncertainty, external disturbance, and actuator effectiveness loss, the controller successfully ensure to achieve the desired objective.

As mentioned in Table 2, and illustrated in the top and the bottom frame of Fig. 4, $(|q_{ev}|, |\Omega|) \leq 2e-2$ is achieved in 20.9 s. Figure 5 top frame exhibits the time evolution of NSFTSM vector, and it is verifiable that in time 8.05 s, $|\sigma_e| \leq 5e-3$ is established. Figure 5 bottom frame illustrates that the control input pattern is within the imposed limitation $|u| \leq 0.2$ N-m; and no sign of chattering is appeared. The steady precision performance is shown in Figs. 4b and 5b. Figure 6 illustrates the estimates of control gains; as expected, the estimate of control gains are attained the higher values than their counterparts of pure condition.

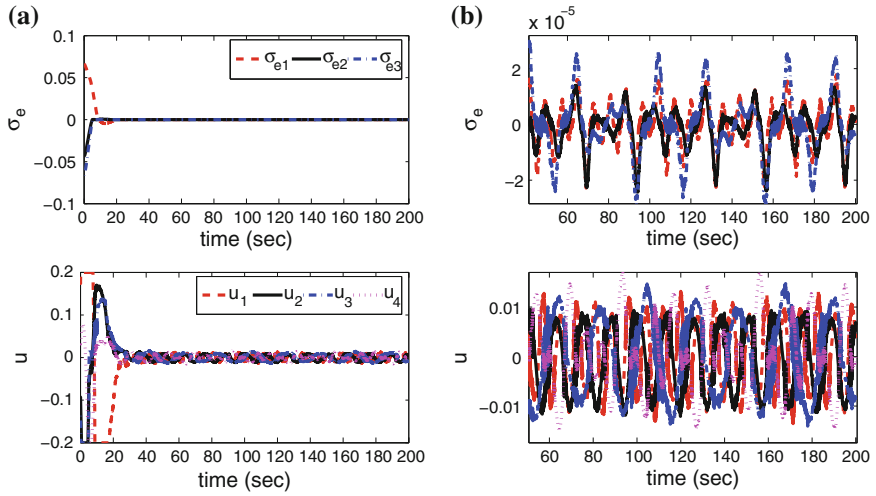

Fig. 5 Stabilization performance Case 2: sliding vectors and control input pattern under uncertainty, disturbance, actuator fault. **a** Sliding vectors and control input. **b** Steady precision

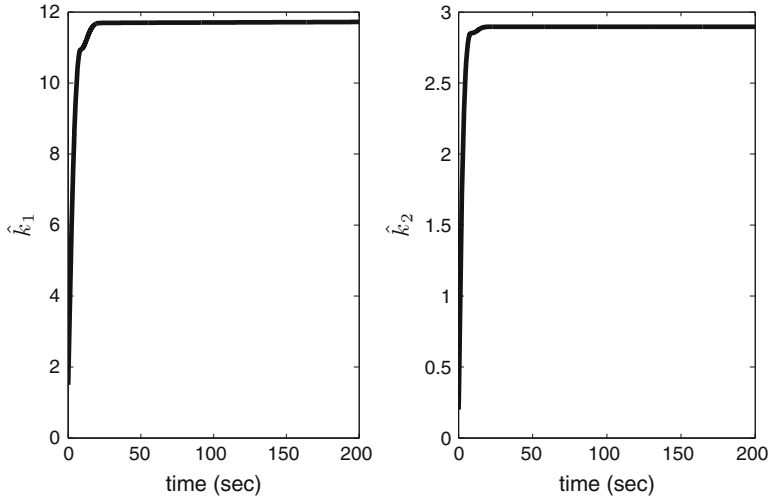

Fig. 6 Stabilization performance Case 2: estimate of control gains

Interestingly, in the pure conditions' control input patterns, the fourth reaction wheel output always satisfy $|u| < 0.2$ N-m, and attain never to the maximum limit ($|u| = 0.2$ N-m). In contrary, for the practical case, the all four reaction wheels output need to attain to the maximum limit. Additionally, in the practical case, the reaction wheels maximum control output is to be required to apply for the longer duration.

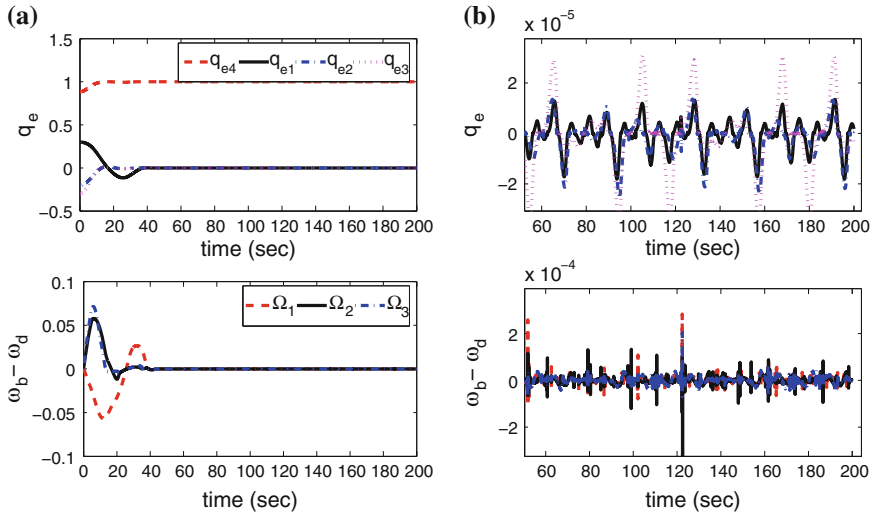

Fig. 7 Controller (22) (Hu et al. 2012) stabilization performance: quaternion and angular velocity pattern under uncertainty, disturbance, actuator fault. **a** Quaternion and angular velocity. **b** Steady precision

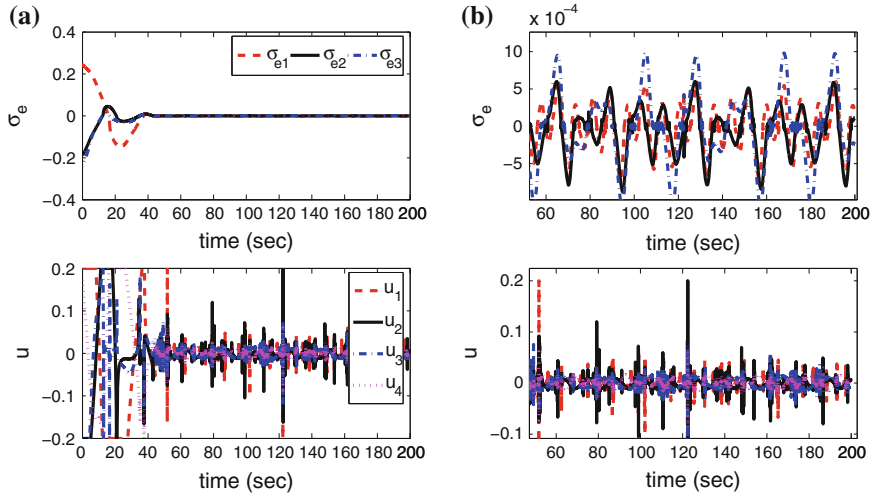

Fig. 8 Controller (22) (Hu et al. 2012) stabilization performance: sliding vectors and control input pattern under uncertainty, disturbance, actuator fault. **a** Sliding vectors and control input. **b** Steady precision

For the comparative analysis, the proposed controller stabilization performance is compared with the controller (22) (Hu et al. 2012). Simulation results to the similar condition are shown in Figs. 7 and 8. The salient points of the proposed controller are the non-singularity, faster convergence speed, and the adaptive law estimated gains. Particularly, the proposed controller ensured to satisfy the criterion $|\sigma_e| \leq 5e\text{-}3$ and $(|q_{ei}|, |\Omega_i|) < (2e\text{-}2, 2e\text{-}2)$ for $i = 1, 2, 3$ in time 8.05 and 20.9 s. respectively; but the controller (22) (Hu et al. 2012) takes 36.81 and 35.42 s. respectively, to satisfy the similar criterion. The steady precision level are almost same for both controller, but the the proposed controller is more quicker in fault tolerant, and it doesn't demand the uncertainty or disturbance bounds to decide the controller's gains.

4.2 Step 2: Spacecraft Attitude Tracking

Further, to examine the tracking performance of controller (12), simulations are conducted on the spacecraft model mentioned in Lu et al. (2013). The nominal component and the uncertain component of inertia matrix are $J_o = [800.027\ 0\ 0;\ 0\ 839.93\ 0;\ 0\ 0\ 289.93]$ and $\delta J = diag[100,\ 100,\ 50]$, respectively. In contrast to stabilization Step, in tracking case the spacecraft attitude is controlled with three reaction wheels only, and the wheels are constrained with torque limit $u(t) = 30$ N-m. The initial conditions of the body frame quaternion and angular velocity are the same as it taken in Step 1 simulations. The initial conditions for the desired frame quaternion and angular velocity are $q_d(0) = [0\ 0\ 0\ 1]^T$ and $\omega_d(t) = 0.05[sin(\pi t \backslash 100)\ sin(2\pi t \backslash 100)\ sin(3\pi t \backslash 100)]^T$, respectively. In this simulation step, in addition to the actuator effectiveness loss the additive fault possibility is also included, and therefore the dynamics of rigid spacecraft is modified to

$$\begin{aligned} J\dot{\omega}_e = {} & (-\omega_e + C\omega_d)^{\times} J(\omega_e + C\omega_d) + J(\omega_e^{\times} C\omega_d - C\dot{\omega}_d) \\ & + (D\ \Delta(t)\ u(t) + E(t)) + d(t). \end{aligned} \tag{35}$$

where $E(t) = [e_1 \quad e_2 \quad e_3]^T$ is the additive fault.

The mathematical model considered for the external disturbance, the actuator effectiveness loss, and the additive fault are as follows

Disturbance:

$$d(t) = [0.1\ sin\ 0.1t\ 0.2\ sin\ 0.2t\ 0.3\ sin\ 0.3t]^T \tag{36}$$

Actuator Effectiveness:

$$\Delta_1 = \begin{cases} 1, & \text{if } t \leq 10\,\text{s}. \\ 0.75 + 0.1sin(0.5t + \pi/3), & \text{if } t > 10\,\text{s}. \end{cases}$$

$$\Delta_2 = \begin{cases} 1, & \text{if } t \leq 10\,\text{s}. \\ 0.75 + 0.1sin(0.5t + 2\pi/3), & \text{if } t > 10\,\text{s}. \end{cases}$$

$$\Delta_3 = \begin{cases} 1, & \text{if } t \leq 10\,\text{s}. \\ 0.75 + 0.1sin(0.5t + \pi), & \text{if } t > 10\,\text{s}. \end{cases} \tag{37}$$

Additive fault:

$$e_i = \begin{cases} 0, & \text{if } t < 15\,\text{s}. \\ 0.1 + 0.05sin(0.5\pi t), & \text{if } t \geq 15\,\text{s}. \\ \text{for } i = 1, 2, 3 \end{cases}$$

4.2.1 Interpretation and Discussion with Comparative Comments on Tracking Performance

By applying the afore-mentioned external disturbance, inertia uncertainty, actuator effectiveness loss, and additive fault, the simulation results for the attitude tracking are shown in Figs. 9 10, 11, and 12.

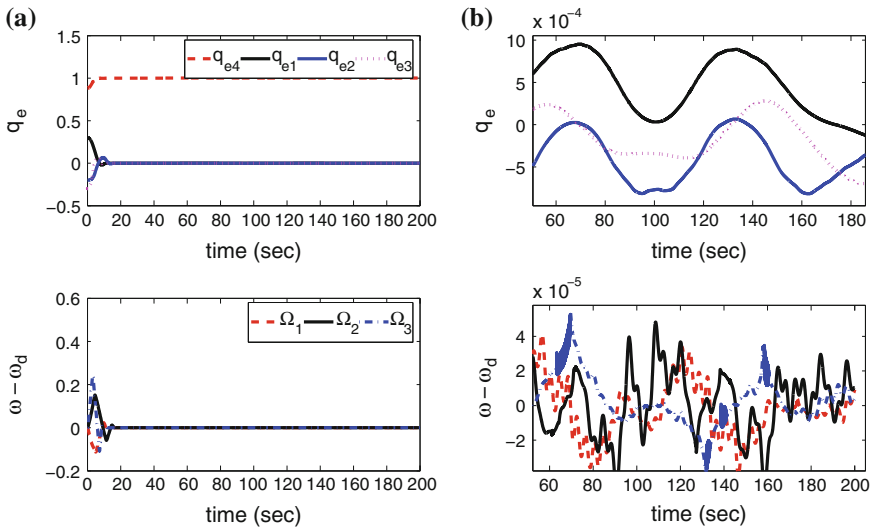

Fig. 9 Tracking performance: quaternion and angular velocity pattern under uncertainty, disturbance, actuator fault. **a** Quaternion and angular velocity. **b** Steady precision

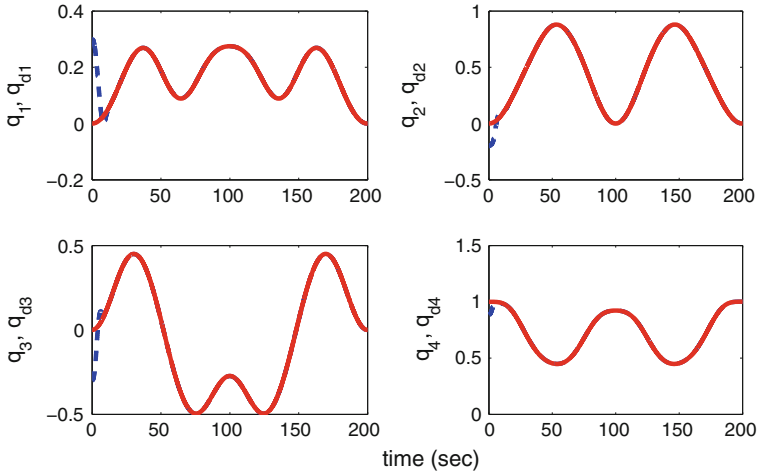

Fig. 10 Tracking performance: quaternion tracking pattern

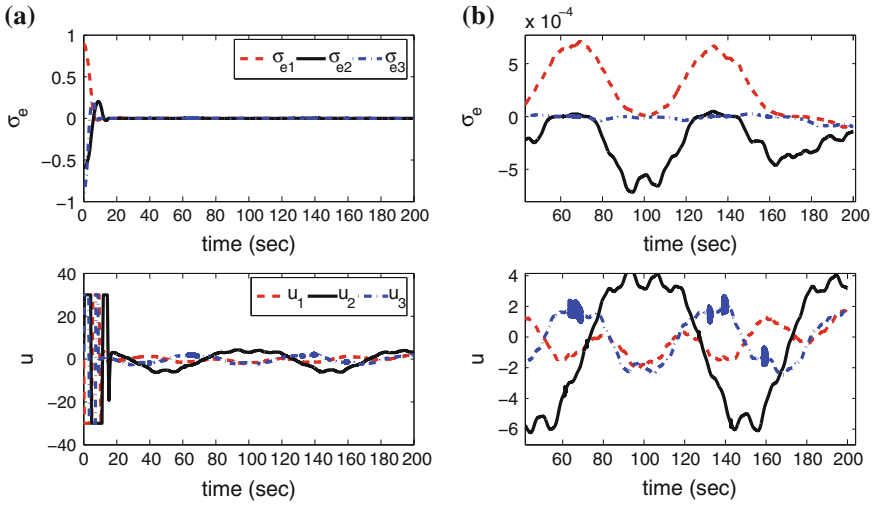

Fig. 11 Tracking performance: sliding vectors and control input pattern under uncertainty, disturbance, actuator fault. **a** Sliding vectors and control input. **b** Steady precision

The error quaternion and the angular velocity tracking errors are portrayed in Fig. 9, it illustrates that the controller is successfully negates the odd effects, and ensures the tracking performance in finite time. Additionally, as mentioned in Table 2, and illustrated in the top and the bottom frame of Fig. 9a, $(|q_{ev}|, |\Omega|) \leq 2e - 2$ is achieved in 13.15 s. For the better lucidity, the quaternion tracking pattern is also shown in Fig. 10, and this also approves the attitude tracking performance. The NSFTSM and the control input time evolution are depicted in Fig. 11, it illustrates

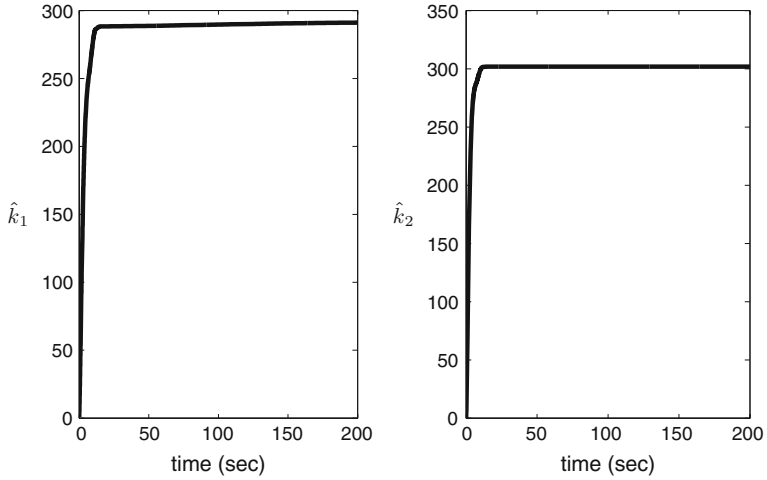

Fig. 12 Tracking performance: estimate of control gains

that NSFTSM vector reached into region $|\sigma_e| < 5e-3$ in time 14.81 s, and the control input is maintained within the defined constraint $|u| \leq 30$ N-m without any sign of chattering. In steady region, the control input is limited within $|u| \leq 4$ N-m. The steady precision for the error quaternion and the angular velocity error, and the NSFTSM vector are shown in Figs. 9b and 11b, respectively; from these illustration and Table 2, it is noted that for attitude tracking, the proposed controller guarantee the steady precision in $|q_{ev}| < 8.80e-4$, $|\Omega| < 3.66e-5$, $|\sigma_e| < 6.62e-5$. Figure 12 illustrates the estimate of control gains.

To compare the performance of the proposed controller (12), the simulation results of the proposed controller and controller (13) (Lu et al. 2013) are scrutinized. The simulation under same initial condition is conducted for the controller (13) (Lu et al. 2013); and the results are shown in Figs.13 and 14. As is mentioned in (Lu et al. 2013), the selected values for the gains are $\tau_i = \sigma_i = 50$. With these gain values, it is verified that finally the controller's gains attained to the level of 10^4.

It is noticed that the proposed controller is to require lesser time to track the desired attitude than to the controller (13) (Lu et al. 2013). In more detail, the controller (13) (Lu et al. 2013) took 30.34 and 29.06 s. to satisfy the criterion $|\sigma_e| \leq 5e$-3 and $(|q_{ei}|, |\Omega_i|) < (2e\text{-}2, 2e\text{-}2)$ for $i = 1, 2, 3$, respectively; in contrary, to satisfy the same criterion, the proposed controller (12) is demanded 14.81 and 13.15 s, respectively. Though, the steady precision for error quaternion and angular velocity error is slightly lower than to the controller (13) (Lu et al. 2013)(*Refer to Table* 2), yet it is acceptable and comes in high precision range. Additionally, in contrary to the controller (13) (Lu et al. 2013), the proposed controller's gains are not selected on any conservative approach, and in fact are being estimated with the proposed adaptive law; hence, even if any unwanted and unaccounted external disturbance and uncertainty surfaced, then also the proposed controller is equipped with adaptive laws to overcome its effect.

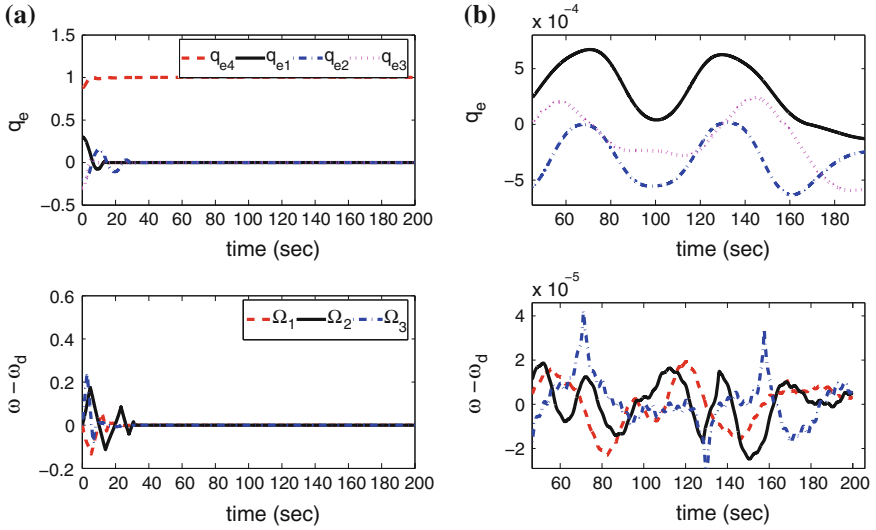

Fig. 13 Controller (13) (Lu et al. 2013) tracking performance: quaternion and angular velocity pattern under uncertainty, disturbance, actuator fault. **a** Quaternion and angular velocity. **b** Steady precision

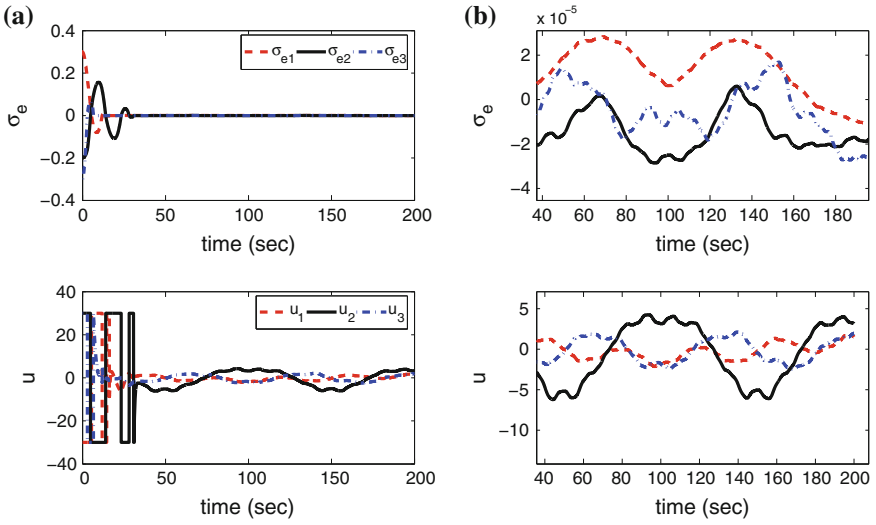

Fig. 14 Controller (13) (Lu et al. 2013) tracking performance: sliding vectors and control input pattern under uncertainty, disturbance, actuator fault. **a** Sliding vectors and control input. **b** Steady precision

5 Conclusion

By using the NSFTSM, a fault-tolerant control law for rigid spacecraft attitude control has been proposed. The proposed control has two components, nominal and adaptive. The adaptive component is designed with aims to ensure quick convergence speed and to eliminate the advance requirements for uncertainty and external disturbance upper bounds. Additionally, by the proposed control, the chattering is eliminated, and the singularity is removed also. The finite-time stability is proved using the Lyapunov stability theorem. The simulation results for attitude stabilization and tracking are reported for two different example spacecraft, respectively, to illustrate the controller efficacy. The shown results reveal that even in presence of inertia uncertainty, external disturbance, and actuator saturation, the controller is able to ensure the fault tolerance, and successfully stabilize and track the desired equilibrium and the desired attitude frame, respectively. In both the stabilization and the tracking case, quick convergence speed and high steady precision is noticed.

Though, the proposed controller gives the required performance for the system considered; in the future control design, to give the most practical solution, actuator dynamics and spacecraft structure flexibility may be include to.

Appendix

To show that $\omega_e = 0$ is not an attractor in reaching phase, apply (12), (13), (14) in (7), and $\bar{L} = 0$, yields

$$\begin{aligned}\dot{\omega}_e = {} & \frac{1}{2\alpha}(M_1 \alpha diag(|q_{ev}|^{\alpha-1}) + M_2)(q_{e4} I_3 + q_{ev}^{\times}) sig^{2-\alpha}\omega_e \\ & -k_1^{'}\sigma_e - k_2^{'} sig^{\gamma}\sigma_e \end{aligned} \tag{38}$$

where, $k_1^{'} = J_o^{-1}\hat{k}_1 \in \Re^{3\times 3}$ and $k_2^{'} = J_o^{-1}\hat{k}_2 \in \Re^{3\times 3}$.
Substituting $\omega_e = 0$, (38) gives

$$\dot{\omega}_e = -k_1^{'}\sigma_e - k_2^{'} sig^{\gamma}\sigma_e, \tag{39}$$

from (39) it is obvious that $\dot{\omega}_e$ is not zero in reaching phase ($\sigma_e \neq 0$). Hence, $\omega_e = 0$ is not an attractor in reaching phase.

References

Bustan, D., Sani, S.K.H., Pariz, N.: Adaptive fault-tolerant spacecraft attitude control design with transient response Control. IEEE/ASME Trans. Mechatron. **19**(4), 1404–1411 (2013)

Ding, S., Li, S.: Stabilization of the attitude of a rigid spacecraft with external disturbances using finite-time control techniques. Aerosp. Sci. Technol. **13**(4–5), 256–265 (2009)

Erdong, J., Zhaowei, S.: Robust controllers design with finite time convergence for rigid spacecraft attitude tracking control. Aerosp. Sci. Technol. **12**(4), 324–330 (2008)

Feng, Y., Yu, X.H., Man, Z.: Non-singular terminal sliding mode control of rigid manipulator. Automatica **38**(12), 2159–2167 (2002)

Haimo, V.T.: Finite time controllers. SIAM J. Control Optim **24**(4), 760–770 (1986)

Hung, J.Y., Gao, W., Hung, J.C.: Variable structure control: a survey. IEEE. Trans. Ind. Electron. **40**(1), 1–12 (1993)

Hu, Q., Huo, X., Xiao, B., Zhang, Z.: Robust finite-time control for spacecraft attitude stabilization under actuator fault. Proc. Inst. Mech. Eng. Part I: J. Syst. Control Eng. **226**(3), 416–428 (2012)

Hu, Q., Xing, Huo, Xiao, B.: Reaction wheel fault tolerant control for spacecraft attittude stabilization with finite time convergence. Int. J. Robust Nonlinear Control **23**(15), 1737–1752 (2012)

Hu, Q., Li, B., Zhang, Aihua: Robust finite-time control allocation in spacecraft attitude stabilization under actuator misalignment. Nonlinear Dyn. **73**(1–2), 53–71 (2013)

Li, S., Wang, Z., Fei, S.: Comments on paper: Robust controllers design with finite time convergence for rigid spacecraft attitude tracking control. Aerosp. Sci. Technol. **15**(3), 193–195 (2011)

Lu, K.,Xia, Y.: Finite-time attitude stabilization for rigid spacecraft. Intern. J. Robust Nonlinear Control (2013). doi:10.1002/rnc.3071

Lu, K., Xia, Y., Fu, M.: Controller design for rigid spacecraft attitude tracking with actuator saturation. Inf. Sci. **220**, 343–366 (2013)

Lu, Kunfeng, Xia, Y., Fu, M.: Finite-time fault-tolerant control for rigid spacecraft with actuator saturations. IET Control Theory Appl. **7**(11), 1529–1539 (2013)

Man, Z., Yu, X.H.: Terminal sliding mode control of MIMO linear systems. IEEE. Trans. on Circuits Syst. **44**(11), 1065–1070 (1997)

Tang, Y.: Terminal sliding mode control of rigid robots. Automatica **34**(1), 51–56 (1998)

Tiwari, P.M., Janardhanan, S., Nabi, M.: A finite time convergent continuous time sliding mode controller for spacecraft attitude control. The 2010 IEEE International Workshop on Variable Structure Systems, 26–28 June 2010, Mexico City, pp. 399–403 (2010). doi:10.1109/VSS.2010.5544630

Tiwari, P.M., Janardhanan, S., Nabi, M.: Spacecraft attitude control using non-singular finite time convergence fast terminal sliding mode. Intern. J. Instrum. Technol. **1**(2), 124–142 (2012)

Tiwari, P.M., Janardhanan, S., Nabi, M.: Rigid spacecraft attitude tracking using finite time sliding mode control. In: The 2014 International Conference on Advances in Control and Optimization of Dynamical Systems, 13–15 March 2014, India, pp. 263–270, (2014). doi:10.3182/20140313-3-IN-3024.00168

Utkin, V.I.: Variable structure systems with sliding modes. IEEE Trans. Autom. Control **22**(2), 212–222 (1977)

Venkataraman, S.T., Gulati, S.: Terminal sliding modes: A new approach. The 1991 International Conference on Advanced Robotics, 19–22 June 1991, Italy, pp. 443–448, (1991). doi:10.1109/ICAR.1991.240613

Vadali, S.R.: Variable-structure control of spacecraft large-Angle Maneuvers. J. Guidance **9**(2), 235–239 (1986)

Wertz, W.: Spacecraft Attitude Determination and Control. In: J. Wertz (ed.), Academic Publishers, New York (1978)

Xiao, B., Hu, Q., Wang, D., Poh, E.K.: Attitude tracking control of rigid spacecrafts with actuator misalignment and fault. IEEE Trans. Control System Technol. **21**(6), 2360–2366 (2013)

Yeh, F.K.: Sliding-mode adaptive attitude controller design for spacecrafts with thrusters. IET Control Theory Appl. **4**(7), 1254–1264 (2010)

Yu, X.H., Man, Z.: On finite time mechanism: Terminal sliding modes. In: The 1996 IEEE International Workshop on Variable Structure Systems, 5–6 Dec 1996, Tokyo, pp. 164–167, (1996). doi:10.1109/VSS.1996.578596

Yu, X.H., Man, Z.: Fast terminal sliding mode control for nonlinear dynamical systems. IEEE. Trans. Circuits Syst. I: Fundam. Theory Appl. **49**(2), 261–264 (2002)

Yu, S., Yu, X.H., Shirinzadeh, B., Man, Z.: Continuous finite-time control for Robotic manipulator with terminal sliding mode. Automatica **41**(11), 1957–1964 (2005)

Yang, L., Yang, J.: Nonsingular fast terminal sliding mode control for nonlinear dynamical systems. Intern. J. Robust Nonlinear Control **21**(16), 1865–1879 (2011)

Zou, A.-M., Kumar, K.D.: Finite-time attitude tracking control for spacecraft using terminal sliding mode and chebyshev neural network. IEEE. Trans. Syst. Man Cybern. **41**(4), 950–963 (2011)

Zhang, A., Hu, Q., Friswell, M.: Finite-time fault tolerant attitude control for over-activated spacecraft subject to actuator misalignment and faults. IET Control Theory Appl. **7**(16), 2007–2020 (2013)